Shiyu Liu
Zhiqiang Wang ✉
Zhenyu Lei

https://doi.org/10.21278/TOF.483058823
ISSN 1333-1124
eISSN 1849-1391

ANALYSIS OF STICK-SLIP CHARACTERISTICS OF AN INCLINED FRICTIONAL CONTACT SYSTEM

Summary

For the purpose of investigating the stick-slip characteristics of the inclined frictional contact interface, a three-dimensional numerical model of a slider-substrate inclined frictional contact system is constructed by using the finite element method, and the state of stick-slip distribution and the dynamic response characteristics of the contact surface are analysed to elucidate the specific vibration mechanism. Combined with the parametric analysis, the control suggestions for the stick-slip vibration are given. The results show that, when the relative motion of the contact interface between the slider and the substrate occurs, the contact surface transitions from the stick-slip state to the slip state. The vibration mechanism of the system can be described as the unsteady vibration form combining stick-slip vibration in the initial stage and slip vibration in the middle and later stages. Compared to the planar frictional contact system, the inclined frictional contact system does not show the stable slip vibration, which is related to the fact that the inclined frictional contact system always has the downward force component along the inclined surface. The parametric analysis reveals that an appropriate reduction in the concentrated force, spring stiffness and frictional coefficient and an increase in the damping coefficient and the base angle can effectively moderate the vibration degree of the slider-substrate system.

Key words: *inclined friction, stick-slip characteristics, finite element method, vibration mechanism, parametric analysis*

1. Introduction

The stick-slip phenomenon exists on the interacting surfaces of objects in contact and is specifically characterised by the development of alternating stick and slip motions. The stick-slip motion may introduce dynamic instability in mechanical systems, leading to abnormal vibration and noise and adversely affecting the normal operation of the system. Therefore, the research on stick-slip characteristics has been one of the important topics in both academia and industry [1]. The vibration caused by the stick-slip phenomenon (i.e. stick-slip vibration) commonly occurs in all kinds of mechanical systems, which is related to the difference between dynamic and static frictional coefficients at the contact interface, and a typical feature of the stick-slip vibration is the emergence of a zero relative velocity state at the contact interface [2, 3]. The stick-slip vibration is closely related to many physical phenomena, such as the musical sound played by a string instrument, the squeaking of the door axle, the noise of the tire when

the vehicle brakes, and the squealing of the railroad wheel-rail system. While the stick-slip vibration can have some positive effects (e.g. pleasant music), non-artificial stick-slip vibration is in most cases not desired and should be avoided as much as possible.

To understand the nature of the stick-slip phenomenon, researchers have developed analytical/numerical models of varying complexity to elucidate stick-slip vibration characteristics. Thomsen and Fidlin [4] derived approximate analytical expressions for conditions, amplitudes and fundamental frequencies of stick-slip and pure slip vibrations using the classical "mass-on-moving-belt" model and showed that the stick phase was linked to the subsequent slip phase by continuity and periodicity conditions. Hong et al. [5] analysed the stick-slip vibration between an oscillator and a crossbeam and found that the long-period stick-slip vibration was mainly affected by the oscillator, while the short-period stick-slip vibration was mainly affected by the axial deformation of the crossbeam. Also, the system would produce a kind of internal resonance when the natural frequency of the oscillator was the same as the natural frequency of the crossbeam. Won et al. [6] investigated the stick-slip vibration of a cantilever beam under the fundamental harmonic excitation, and the results revealed that the occurrence of the stick-slip vibration depended on the excitation amplitude and frequency, and the occurrence of the stick-slip vibration was related to the modal characteristics of the beam. Maegawa and Itoigawa [7] proposed reasonable design conditions for dynamic vibration absorbers to achieve steady sliding without stick-slip and solved the boundary conditions for occurrence and non-occurrence of stick-slip by combining the fixed-point theory and the stick-slip dynamics theory. He et al. [8] analysed the energy dissipation characteristics of a frictional damper due to the stick-slip vibration under the condition of harmonic excitation and found that the intermediate range of the normal contact force (in the stick-slip state) could provide the best dissipation performance. Kang et al. [9] studied the stick-slip vibration of a discrete system under the interaction of a nonlinear smooth frictional profile with a translational energy source by applying the numerical time integration and analytical methods. The results indicated that the steady state response of the coupled oscillator could be manifested in two different vibration modes depending on the mode separation, i.e. the mode-merged vibration and the mode-separated vibration. Zhu et al. [10] discussed the effect of constant normal force and alternating normal force on the stick-slip vibration characteristics for different coefficients of dynamic and static friction. The results demonstrated that the frictional system had richer dynamic vibration characteristics under the action of alternating normal force and that increasing the difference between dynamic and static frictional coefficients increased the possibility of the system to slide into chaos.

Meanwhile, in order to examine the validity of stick-slip theoretical models, experimental analysis has also gradually become a major research approach. Clark et al. [11] experimentally investigated the frictional behaviour of a two-dimensional slider as it was slowly pulled over a particle substrate consisting of photoelastic disks and found that the stick-slip behaviour was enhanced as vibration frequency increased. Abdo et al. [12] analysed the variation of the stick-slip amplitude on a mild steel disc with variations in vibration frequency and relative humidity and concluded that the rate of the reduction in the stick-slip amplitude was related to vibration frequency and relative humidity. Further, Abdo and Zaier [13] investigated the frictional stability of different types of soft and hard materials and found that the stick-slip amplitude depended on the type of material and that the stick-slip amplitude decreased with an increase in the vibration amplitude. Leus and Abrahamowicz [14] presented experimental results on the effect of longitudinal tangential vibration on the stick-slip phenomenon, and the analysis showed that the longitudinal tangential vibration helped to reduce or even completely eliminate the stick-slip phenomenon. Zhou et al. [15] proposed a stick-slip characterisation test method based on a closed-loop serving system with the linear motor positioning and concluded that reducing the mass of the bench, increasing the spring stiffness, decreasing the difference between the coefficients of dynamic and static friction, and increasing the tensile velocity could all inhibit the stick-slip phenomenon. Gong [16] tested the stick-slip features of mica, quartz, and single crystal silicon

wafers under interfacial frictional conditions using the atomic force microscope and found that the stick-slip frequency and the stick-slip vibration amplitude were not the same in different materials.

Based on the literature review, it can be seen that the existing research on the stick-slip phenomenon is extensive and relatively detailed. However, most of the research has been carried out and implemented in planar frictional contact systems and analyses of stick-slip properties of inclined frictional contact interfaces have been rarely reported. Given that, this paper focuses on the stick-slip behaviour of an inclined frictional contact system. Since the finite element method can fully consider the elastic deformation and material properties of objects in contact, the method includes a detailed description of stick-slip features of the surfaces in contact. The sections of this paper are organized as follows: firstly, using the finite element method, a three-dimensional numerical model of a slider-substrate inclined frictional contact system is established; then, the numerical model is utilized to execute calculations to analyse the stick-slip distribution state and dynamic response characteristics of the inclined frictional contact interface so as to explain the stick-slip vibration mechanism of the system; finally, a parametric analysis of the inclined frictional contact system is carried out and corresponding recommendations related to the control of the stick-slip vibration are given.

2. Numerical model

2.1 Model establishment

Based on the finite element theory, a three-dimensional numerical model of a slider-substrate inclined frictional contact system is constructed by using ABAQUS software. The system mainly consists of a slider, a substrate, a spring and a damper, as shown in Figure 1. The slider is a square cube with side lengths of 10 mm; the substrate is a triangular prism with right-angled triangles on its sides, the lengths of right-angled sides are both 50 mm, i.e. the base angle is 45° and the height of the prism is 20 mm. The bottom surface of the slider is in contact with the inclined surface of the substrate and the initial position of the centre of the bottom surface of the slider is located and cantered at the three-quarter position of the inclined surface of the substrate. The contact between the slider and the substrate is performed using a face-to-face contact algorithm with a finite slip formulation, where the normal behaviour is characterised using the "hard" contact and allowing objects to separate after contact. The tangential behaviour is characterised by using the "penalty" function frictional formulation with a frictional coefficient of 0.35 [17-18]. The upper surface of the slider is connected to the fixed point by means of a spring and a damper, as shown in the side view presented in Figure 1. The material parameters of the slider and the substrate and the connection parameters of the slider and the fixed point are shown in Table 1.

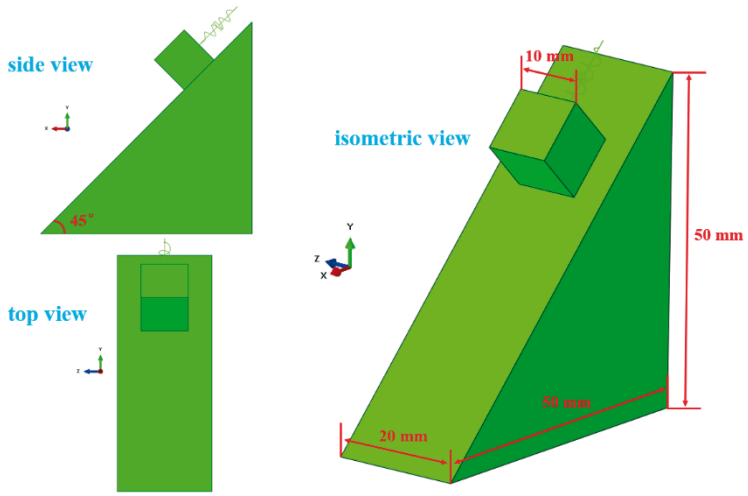

Fig. 1 Numerical model

The mesh size of the contact surfaces of the numerical model is 0.5×0.5 mm, as shown in Figure 2(a). The total number of elements is 78,080 and the total number of nodes is 84,783. Since the mesh size has a certain influence on the calculation results, the above mesh size is chosen based mainly on the mesh dependency analysis of the calculation results. The maximum normal contact stress is used to represent the response variable of the calculation results and its variation curve under different mesh sizes is shown in Figure 2(b). From Figure 2(b), it can be seen that when the mesh size is less than 0.75, the variation of the maximum normal contact stress curve tends to decrease, i.e. the variation of its value tends to be stable, therefore, in consideration of the calculation accuracy and calculation efficiency, the mesh size of 0.5 mm is chosen here.

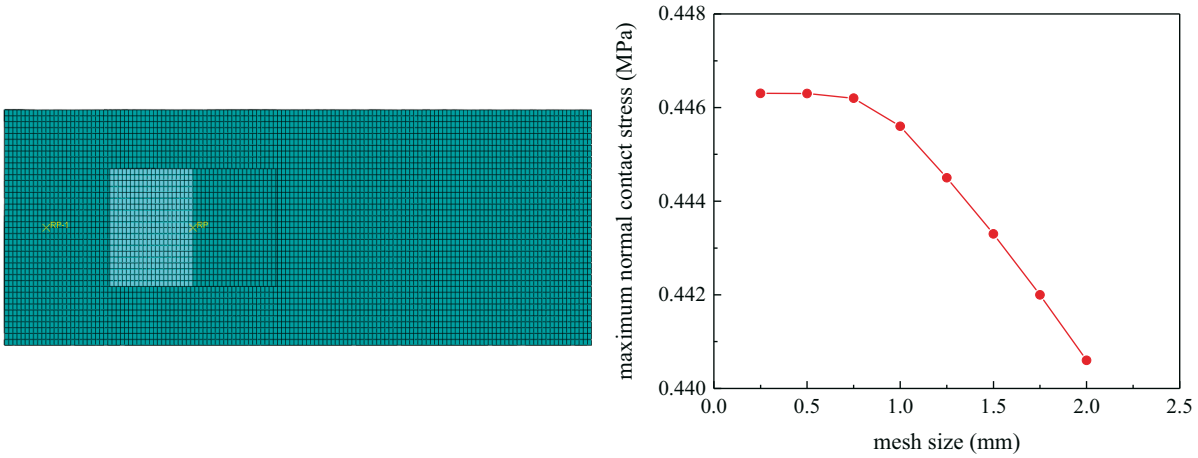

(a) Mesh size of contact surfaces

(b) Variation of maximum normal contact stresses with mesh sizes

Fig. 2 Mesh size of contact surfaces and dependency curve of the mesh size

Table 1 Parameter values of the numerical model

Parameter		Value
Slider/substrate	Density (kg/m^3)	7,800
	Elastic modulus (Pa)	2.1×10^{11}
	Poisson's ratio	0.3
Spring stiffness (N/mm)		1
Damping coefficient (Ns/mm)		1

The boundary conditions of the numerical model are set as follows: the bottom surface (20 mm × 50 mm) and the back surface (20 mm × 50 mm) of the substrate are fixed constraints and there are no other constraints. The load conditions are set as follows: the slider as a whole is subjected to a concentrated force F in the -y direction with an amplitude of 10 N and there are no other loads. Taking the contact surface of the slider as the object of analysis, The forces acting on the slider can be decomposed as: (1) the concentrated force component F_t downward along the contact surface; (2) the concentrated force component F_n perpendicular to and downward from the contact surface; (3) the frictional force F_f provided by the substrate contact surface; (4) the support reaction force F_r provided by the substrate contact surface, as shown in Figure 3. The relationship between F_f and F_n is expressed as follows:

$$F_f \le \mu F_n \tag{1}$$

where μ is the frictional coefficient. F_t and F_n can be further represented by F :

$$\begin{cases} F_t = F\sin\alpha \\ F_n = F\cos\alpha \end{cases} \tag{2}$$

where α is the base angle. From Eqs. (1) and (2), the maximum value $F_{f\max}$ of F_f can be obtained as:

$$F_{f\max} = \mu F\cos\alpha \tag{3}$$

Dividing F_t by $F_{f\max}$ gives:

$$\frac{F_t}{F_{f\max}} = \frac{F\sin\alpha}{\mu F\cos\alpha} = \frac{\tan\alpha}{\mu} \tag{4}$$

When $\frac{\tan\alpha}{\mu} > 1$, i.e. $\alpha > \arctan 0.35 \approx 19.29°$, the slider has the ability to move down the incline. In the numerical model presented in this section, α is 45°, therefore, the contact interface satisfies the condition of occurrence of relative motion.

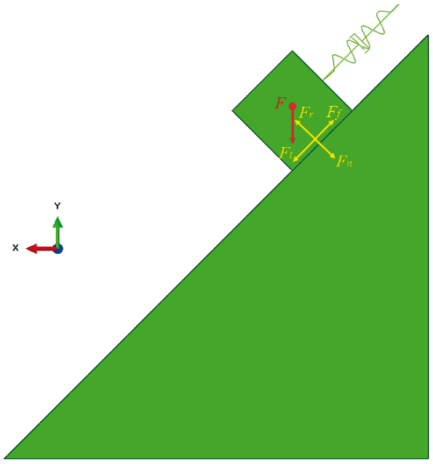

Fig. 3 Forces acting on the contact surface of the slider

2.2 Model verification

In this section, with reference to the finite element model established in Section 2.1, the corresponding rigid body motion equation is established using the analytical method to verify the validity of the finite element model, as shown in Eq. (5):

$$m\ddot{y}(t) + c\dot{y}(t) + ky(t) = F \tag{5}$$

where, m is the slider mass, which is F_n / g (g is the gravity acceleration taken as 9.8 m/s^2); c is the damping coefficient; k is the spring stiffness; F is the external force which is $(F_t - \mu F_n)$ when the slider moves downward along the incline, otherwise 0; t is the calculation time; y, $\dot{y}$ and $\ddot{y}$ are the slider displacement, velocity and acceleration along the downward incline (positive direction), respectively. With the slider displacement as the output variable, the slider displacement curves corresponding to the analytical method and the finite element method can be obtained by calculation, as shown in Figure 4.

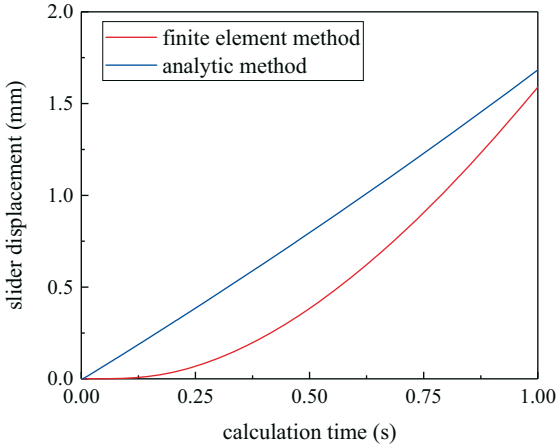

Fig. 4 Slider displacement curves

From Figure 4, it can be seen that during the motion of the slider, compared with the slider displacement obtained by the analytical method, the slider displacement obtained by the finite element method is relatively small at the same time, which is related to the elastic deformation of the objects in contact. With an increase in the slider motion time, the difference between the slider displacements obtained by the two methods tend to decrease. Generally, the results shown in Figure 4 indicate that the numerical model established by the finite element method is feasible and relatively more accurate.

3. Analysis of contact stick-slip characteristics

In this section, by using the numerical model established in Section 2 to perform calculations, the variation process of the stick-slip distribution on the inclined frictional contact surface as well as the dynamic response characteristics of the system are analysed, with a view to elucidating the mechanism of the stick-slip vibration of the system.

3.1 Stick-slip distribution characteristics

When the relative motion of the contact interface between the slider and the substrate occurs, the variation process of the stick-slip distribution state on the contact surface is shown in Figure 5. Figure 5 gives the diagrams of stick-slip states of the contact surface at 10 equally spaced moments (corresponding to calculation moments of 0 s, 0.1 s, 0.2 s, 0.3 s, 0.4 s, 0.5 s, 0.6 s, 0.7 s, 0.8 s, and 0.9 s). It can be seen that at moments 1 and 2, the contact surface is in the stick-slip state (i.e. the coexistence of stick and slip regions), while at moments 3~10, the contact surface is in the slip state. The variation process of the stick-slip state shown in Figure 5 shows that the contact surface undergoes a transition from the stick-slip state to the slip state, and with the increase in time, the slip state completely occupies the contact area for most of the time (calculated for 1.0 s), while the stick state ceases to exist.

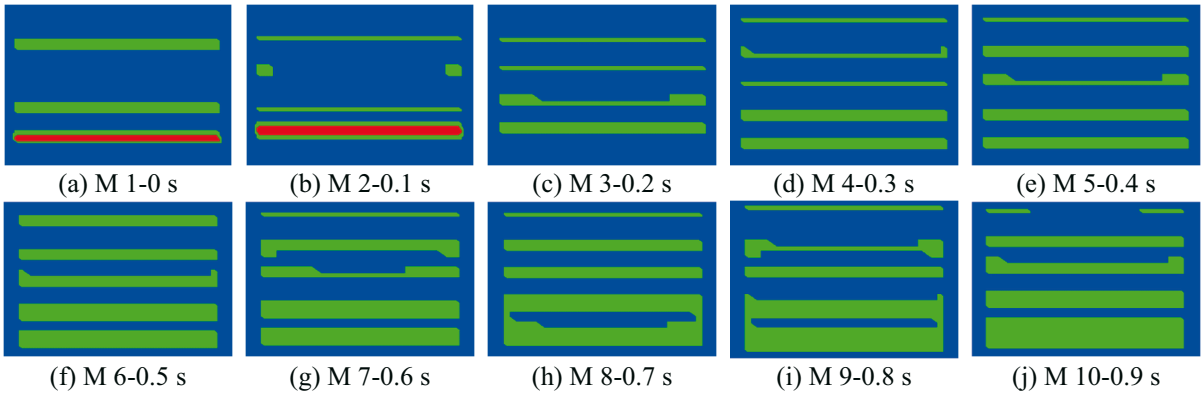

Fig. 5 Stick-slip distribution states (red indicates stick, green indicates slip, blue indicates no contact, M means moment)

The contact areas in the stick-slip and slip states corresponding to moments 2 and 3 are shown in Figure 6. By comparison, it can be seen that the contact area in the slip state corresponding to moment 3 is larger than that in the stick-slip state corresponding to moment 2, which is related to the form of motion of the slider at a particular moment. Similarly, the contact stress diagrams corresponding to moments 2 and 3 are given in Figures 7~8, where Figure 7 is the normal contact stress diagram and Figure 8 is the tangential (along the inclined direction) contact stress diagram. From Figure 7, it is obvious that the normal contact stress in the slip state is larger than that in the stick-slip state, and the maximum value of the normal contact stress in the slip state (0.322 MPa) is about 1.193 times that of the maximum value of the normal contact stress in the stick-slip state (0.270 MPa). From Figure 8, it is clear that although the maximum tangential contact stress in the slip state (0.113 MPa) is the same as that in the stick-slip state (0.113 MPa), the resultant tangential contact stress in the slip state is larger than that in the stick-slip state (the amplitude of the tangential contact stress in the slip state is relatively larger).

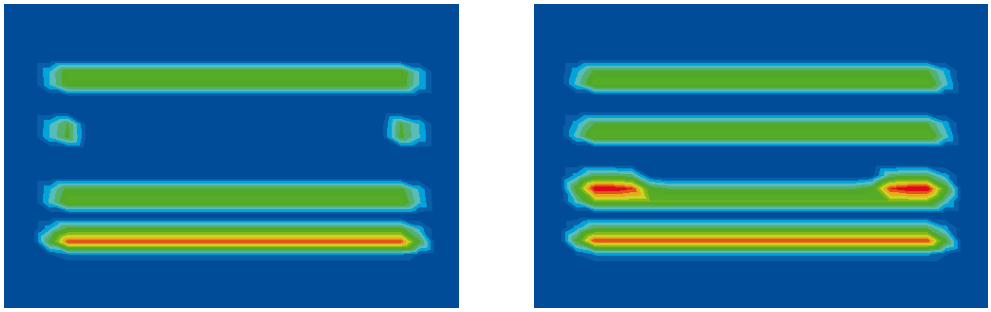

(a) Contact area in the stick-slip state (b) Contact area in the slip state

Fig. 6 Contact areas

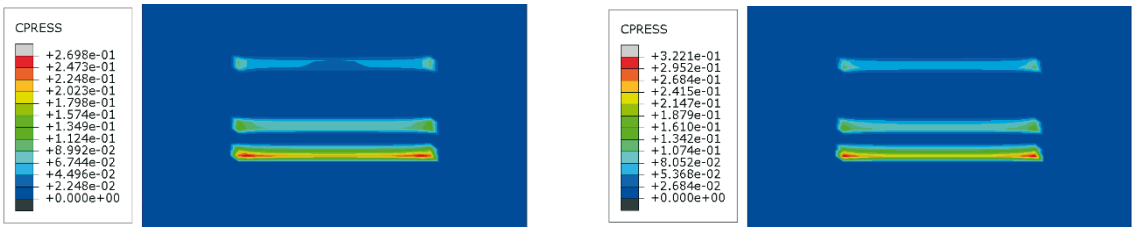

(a) Normal contact stress in the stick-slip state (MPa) (b) Normal contact stress in the slip state (MPa)

Fig. 7 Normal contact stresses

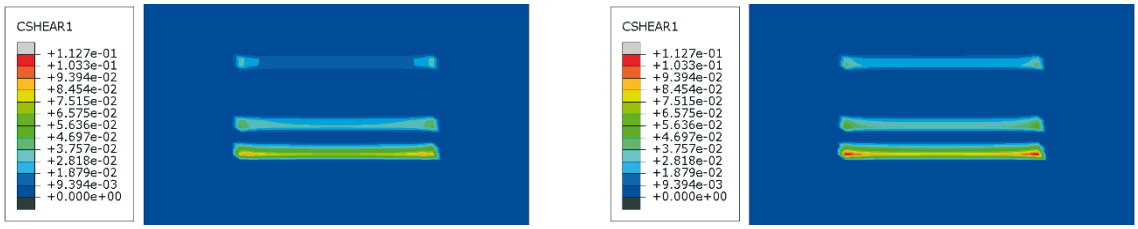

(a) Tangential contact stress in the stick-slip state (MPa) (b) Tangential contact stress in the slip state (MPa)

Fig. 8 Tangential contact stresses

According to Figures 7~8, it can be seen that the force acting on the contact surface in the slip state is larger in amplitude than the corresponding force in the stick-slip state. Since the contact force is directly related to the vibration condition of the system, the dynamic response

of the system in the slip state may be more drastic. In the following section, the dynamic response of the system will be analysed in order to investigate the stick-slip vibration mechanism of the system.

3.2 Dynamic response characteristics

This section focuses on the dynamic response characteristics of the slider-substrate system. The frictional response curve of the contact interface during the motion of the slider is shown in Figure 9.

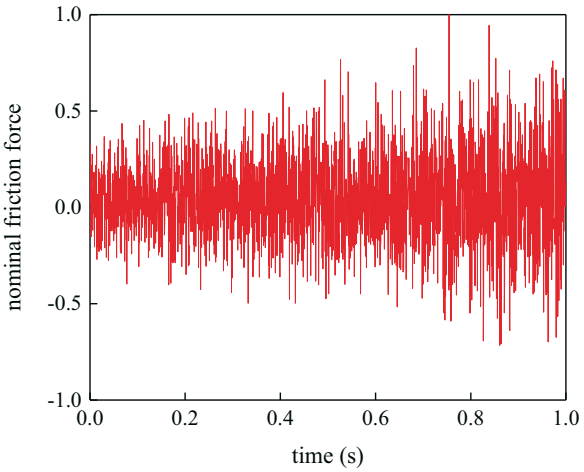

Fig. 9 Time-domain curve of the nominal frictional force

It should be noted that the frictional time-domain curve in Figure 9 was normalized (i.e. it is the nominal frictional force) for ease of analysis. As can be seen from Figure 9, the vibration amplitude of the nominal frictional force increases gradually with an increase in the slider motion time, and the vibration degree tends to intensify, which indicates that the unstable vibration of the slider-substrate system occurs. By establishing a local Cartesian coordinate system as shown in Figure 10 and transforming the calculation results to this coordinate system, three-direction (x, y, and z) acceleration curves of the slider node during the motion process can be obtained, as shown in Figure 11. Based on Figure 11, it can be seen that the slider experiences irregular reciprocating vibrations during its motion, especially in the x-direction (i.e. the direction of the slider's motion).

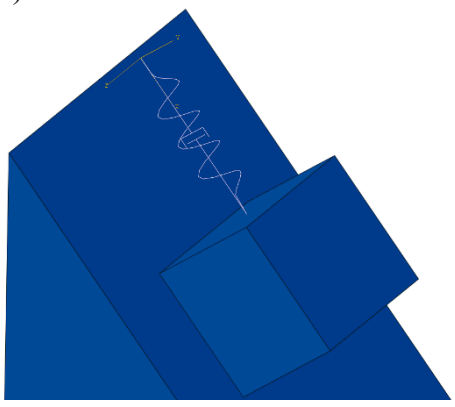

Fig. 10 Local Cartesian coordinate system

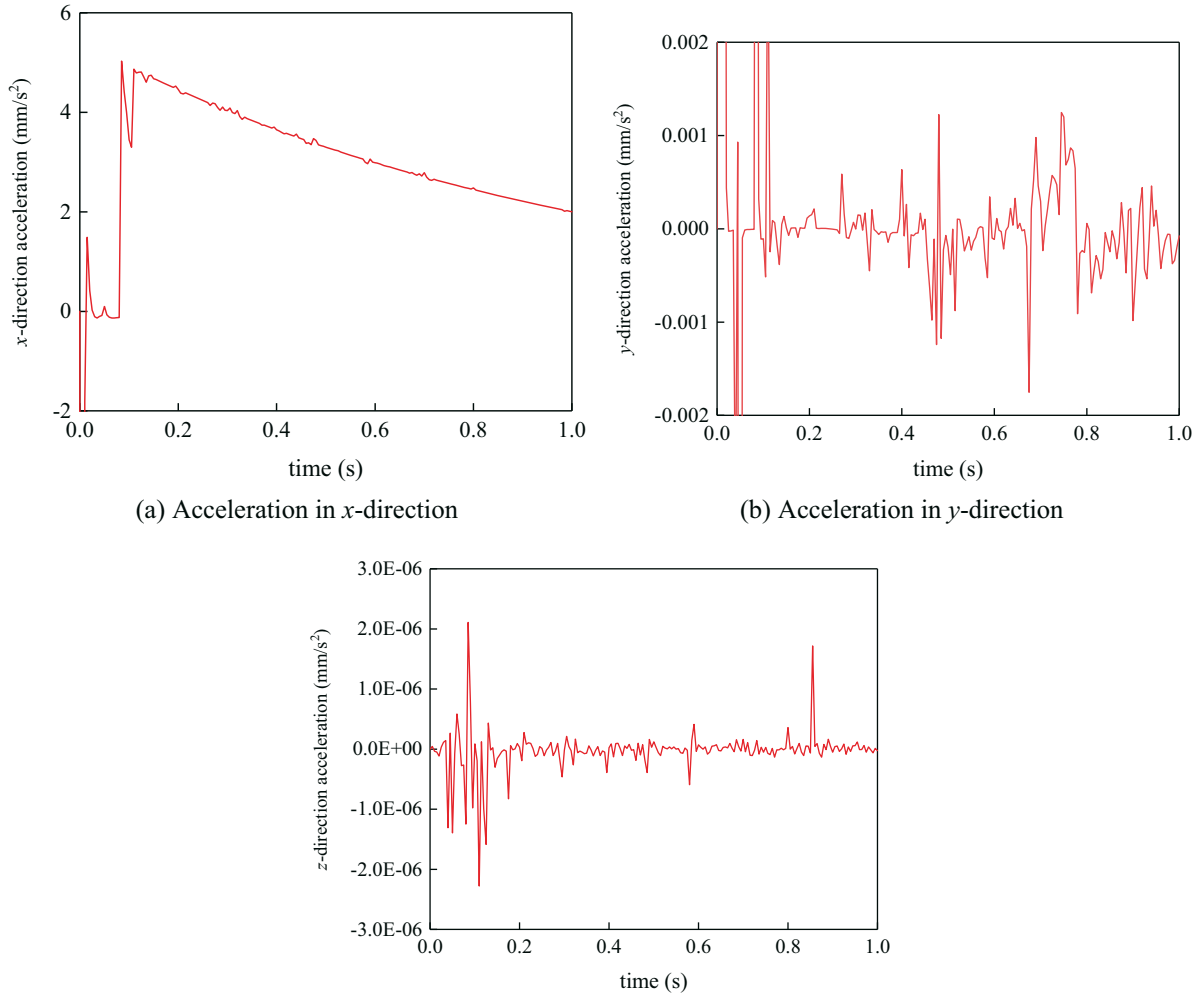

(a) Acceleration in *x*-direction

(b) Acceleration in *y*-direction

(c) Acceleration in *z*-direction

Fig. 11 Acceleration curves of the slider node

Figures 9 and 11 show that the slider-substrate system undergoes unstable vibrations; however, the exact vibration mechanism is not yet known. Since the relative velocity of the contact interface can reflect the vibration form of the system to some extent [19-21], the vibration mechanism of the slider-substrate system is analysed in this section by taking the velocity curve of the slider node as an example. Figure 12 shows the velocity curve in the *x*-direction of the slider node, and it is easy to see that the vibration response of the slider-substrate system consists of the stick-slip vibration phase (i.e. the phase with velocity of 0 in Figure 12) and the slip vibration phase (i.e. the part following the stick-slip vibration phase in Figure 12) throughout the entire time history, where the duration of the stick-slip vibration is about 0.1 s, while the duration of the slip vibration is about 0.9 s, indicating that the slip vibration occupies most of the time history, which is consistent with the results shown in Figure 5.

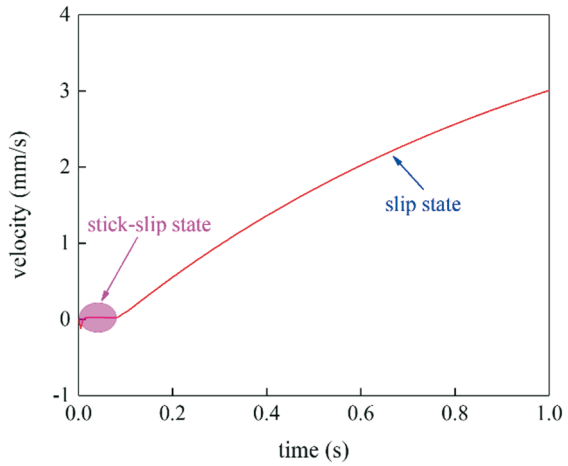

Fig. 12 Velocity curve of the slider node in *x*-direction

Further, the vibration mechanism of the slider-substrate inclined frictional contact system can be represented by Figures 9 and 12 as a form of unsteady vibration of the system combining the stick-slip vibration in the initial stage and the slip vibration in the middle and later stages. Compared to the planar frictional contact system, the inclined frictional contact system does not show stable slip vibration (whereas stable slip vibration is one of the main manifestations of the planar frictional contact system in the slip phase [1]), which is related to the fact that the inclined frictional contact system has always a downward force component along the inclined surface (only for the case of the interface undergoing relative motion, not considering the stationary case).

4. Parametric analysis of stick-slip vibration

Based on the understanding of the vibration mechanism of the system, the parametric analysis of the system response is carried out in this section in an attempt to achieve an effective control of the stick-slip vibration by employing the control variable method, where the variable parameters considered include the concentrated force, the spring stiffness, the damping coefficient, the frictional coefficient, and the base angle.

4.1 Parametric analysis-concentrated force

The nominal frictional force at the contact interface is used to represent the dynamic response of the system, the concentrated force is set to take the values of 5 N and 10 N, and the values of other parameters are kept constant. Then, the numerical model constructed in Section 2 is utilized to execute the calculations and the obtained time-domain curves of the nominal frictional forces for different concentrated force conditions are shown in Figure 13.

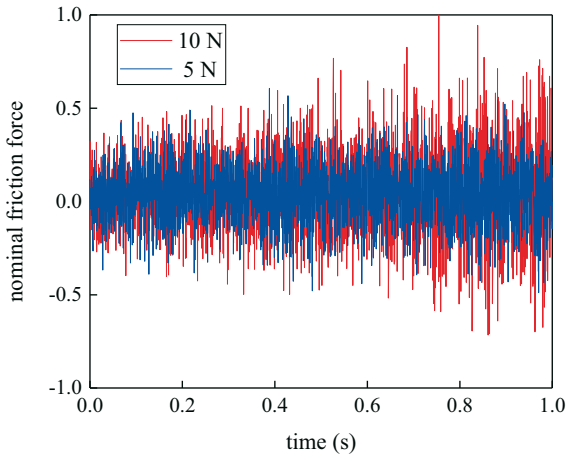

Fig. 13 Time-domain curves of nominal frictional forces – different concentrated force conditions

Figure 13 shows that the vibration amplitude of the nominal frictional force tends to increase with an increase in the concentrated force, indicating that the increase in the concentrated force will contribute to the increase in the vibration degree of the slider-substrate system. Therefore, an appropriate reduction in the amplitude of the concentrated force can moderate the stick-slip (or slip) vibration of the system.

4.2 Parametric analysis-spring stiffness

Set the spring stiffness in the numerical model as 0.5 N/mm and 1 N/mm and keep the values of other parameters constant. Through simulation, the time-domain curves of nominal frictional forces under different spring stiffness conditions can be obtained, as shown in Figure 14.

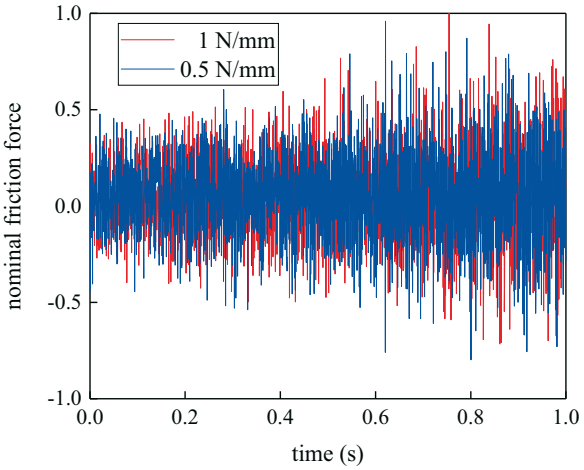

Fig. 14 Time-domain curves of nominal frictional forces – different spring stiffness conditions

Based on Figure 14, it can be found that an increase in the spring stiffness in the numerical model will make the vibration amplitude of the nominal frictional force at the contact interface increase, which suggests that the increase in the spring stiffness will also exacerbate the vibration degree of the slider-substrate system. Therefore, a proper reduction in the spring stiffness can moderate the system stick-slip (or slip) vibration to some extent.

4.3 Parametric analysis – damping coefficient

By setting the damping coefficient in the numerical model as 0.5 Ns/mm and 1 Ns/mm, and keeping the other parameters unchanged, and then executing the numerical calculations, the obtained time-domain curves of nominal frictional forces under different damping coefficient conditions are shown in Figure 15.

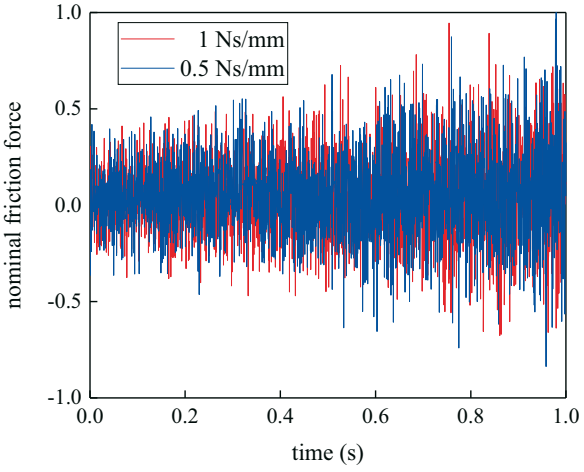

Fig. 15 Time-domain curves of nominal frictional forces – different damping coefficient conditions

As can be seen from Figure 15, unlike the effect of the concentrated force and spring stiffness, an increase in the damping coefficient reduces the vibration amplitude of the nominal frictional force, indicating that an appropriate increase in the damping coefficient in the numerical model can moderate the vibration degree of the system and establish an effective control of the system stick-slip (or slip) vibration.

4.4 Parametric analysis-frictional coefficient

By setting the values of frictional coefficients in the numerical model as 0.25 and 0.35 and keeping other parameters unchanged, the calculated time-domain curves of the nominal frictional forces under different frictional coefficients are shown in Figure 16.

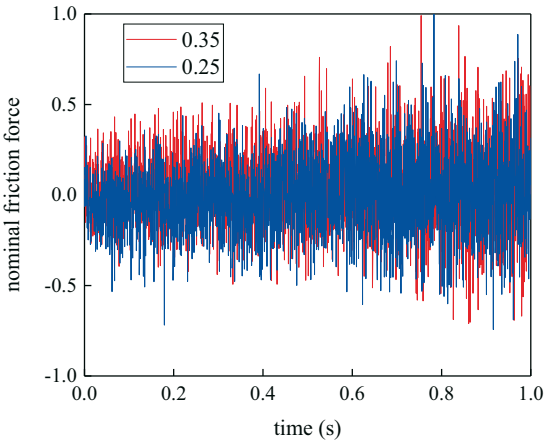

Fig. 16 Time-domain curves of nominal frictional forces – different frictional coefficient conditions

From Figure 16, it can be seen that when the interfacial frictional coefficient is increased in the numerical model, the vibration amplitude of the nominal frictional force tends to increase, demonstrating that the increase in the frictional coefficient will exacerbate the vibration degree of the system. Therefore, in order to control the system stick-slip (or slip) vibration, reducing the interfacial frictional coefficient is a more appropriate choice.

4.5 Parametric analysis-base angle

By adjusting the numerical model and setting the base angles as 45° (original model) and 60° (the bottom right-angled side of the substrate is 50 mm and the inclined side is adjusted to 100 mm; the fixed point is adjusted so that the connecting spring and the damper are parallel to the inclined surface; other relevant parameters are adjusted accordingly) and keeping the values of other parameters unchanged, the calculated time-domain curves of the nominal frictional forces under different base angles are shown in Figure 17.

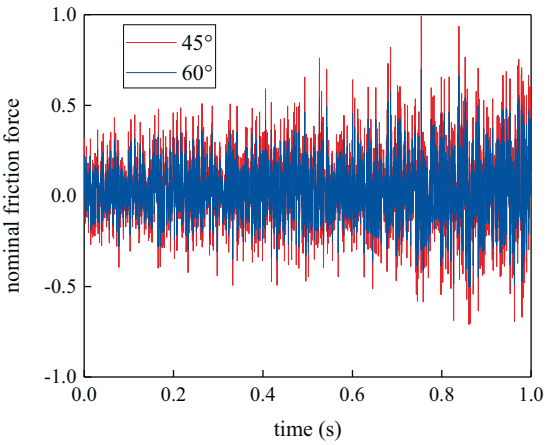

Fig. 17 Time-domain curves of nominal frictional forces – different base angle conditions

From Figure 17, it can be seen that when the base angle in the numerical model is increased, the vibration amplitude of the nominal frictional force tends to decrease, demonstrating that the increase in the base angle will weaken the vibration degree of the system. Therefore, an appropriate increase in the base angle can provide some reference for mitigating the stick-slip (or slip) vibration of the system.

5. Conclusions

In this paper, a three-dimensional numerical model of a slider-substrate inclined frictional contact system is established by using the finite element method. The model is used to study the stick-slip distribution and dynamic response characteristics of the inclined frictional contact interface, so as to explain the vibration mechanism of the system. Further, a parametric analysis of the inclined frictional contact system is carried out and recommendations for the control of stick-slip vibration are given accordingly. The main conclusions are as follows:

(1) When relative motion of the contact interface between the slider and the substrate occurs, the contact surface transitions from the stick-slip state to the slip state, and as the time increases, the slip state completely occupies the contact area for most of the time, while the stick state ceases to exist. At the same time, the force on the contact surface in the slip state is larger in amplitude than the corresponding force in the stick-slip state.

(2) The vibration mechanism of the slider-substrate inclined frictional contact system takes the unsteady vibration form of the system combining the stick-slip vibration in the initial stage and the slip vibration in the middle and later stages. Compared to the planar frictional contact system, which has stable slip vibration, the inclined frictional contact system does not have stable slip vibration, which is related to the fact that the inclined frictional contact system always has a downward force component along the inclined surface.

(3) The parametric analysis of the stick-slip vibration shows that in the numerical model, an appropriate reduction in the concentrated force, spring stiffness and interfacial frictional coefficient and an increase in the damping coefficient and base angle can moderate the vibration degree of the slider-substrate system to a certain extent.

REFERENCES

[1] Won, H.I.; Chung, J. Stick-slip vibration of an oscillator with damping: *Nonlinear Dynamics* **2016**, 86(1), 257-267. https//doi.org/10.1007/s11071-016-2887-x

[2] Nosyreva, E.P.; Molinari, A. Analysis of nonlinear vibrations in metal cutting: *International Journal of Mechanical Sciences* **1998**, 40(8), 735-748. https//doi.org/10.1016/S0020-7403(97)00110-0

[3] Liu, X.B.; Vlajic, N.; Long, X.H.; Meng, G.; Balachandran, B. Nonlinear motions of a flexible rotor with a drill bit: stick-slip and delay effects: *Nonlinear Dynamics* **2013**, 72(1-2), 61-77. https//doi.org/10.1007/s11071-012-0690-x

[4] Thomsen, J.J.; Fidlin, A. Analytical approximations for stick-slip vibration amplitudes: *International Journal of Non-Linear Mechanics* **2003**, 38(3), 389-403. https//doi.org/10.1016/S0020-7462(01)00073-7

[5] Hong, J.G.; Kim, J.; Chung, J. Stick-slip vibration of a moving oscillator on an axially flexible beam: *Journal of Mechanical Science and Technology* **2020**, 34(2), 541-553. https//doi.org/10.1007/s12206-020-0102-y

[6] Won, H.I.; Lee, B.; Chung, J. Stick-slip vibration of a cantilever beam subjected to harmonic base excitation: *Nonlinear Dynamics* **2018**, 92(4), 1815-1828. https//doi.org/10.1007/s11071-018-4164-7

[7] Maegawa, S.; Itoigawa, F. Design method for suppressing stick-slip using dynamic vibration absorber: *Tribology International* **2019**, 140, 105866. https//doi.org/10.1016/j.triboint.2019.105866

[8] He, B.B.; Ouyang, H.J.; He, S.W.; Ren, X.M. Stick-slip vibration of a friction damper for energy dissipation: *Advances in Mechanical Engineering* **2017**, 9(7), 1687814017713921. https//doi.org/10.1177/1687814017713921

[9] Kang, J.; Krousgrill, C.M.; Sadeghi, F. Oscillation pattern of stick-slip vibrations: *International Journal of Non-Linear Mechanics* **2009**, 44(7), 820-828. https//doi.org/10.1016/j.ijnonlinmec.2009.05.002

[10] Zhu, Y.G.; Wang, R.L.; Xiang, Z.Y.; Mo, J.L.; Ouyang, H.J. The effect of dynamic normal force on the stick-slip vibration characteristics: *Nonlinear Dynamics* **2022**, 110(1), 69-93. https//doi.org/10.1007/s11071-022-07614-0

[11] Clark, A.H.; Behringer, R.P.; Krim, J. Vibration can enhance stick-slip behavior for granular friction: *Granular Matter* **2019**, 21(3), 55. https//doi.org/10.1007/s10035-019-0895-5

[12] Abdo, J.; Tahat, M.; Abouelsoud, A.; Danish, M. The effect of frequency of vibration and humidity on the stick-slip amplitude: *International Journal of Mechanics and Materials in Design* **2010**, 6(1), 45-51. https//doi.org/10.1007/s10999-010-9117-3

[13] Abdo, J.; Zaier, R. A novel pin-on-disk machine for stick-slip measurements: *Materials and Manufacturing Processes* **2012**, 27(7), 751-755. https//doi.org/10.1080/10426914.2011.648702

[14] Leus, M.; Abrahamowicz, M. Experimental investigations of elimination the stick-slip phenomenon in the presence of longitudinal tangential vibration: *Acta Mechanica et Automatica* **2019**, 13(1), 45-50. https//doi.org/10.2478/ama-2019-0007

[15] Zhou, W.P.; Yuan, L.B.; Ren, R.; Zhang, W.; Mao, J.H. Stick-slip experimental method based on closed loop positioning system: *Journal of Xi'an Jiaotong University* **2011**, 45(8), 113-117.

[16] Gong, Z.L. Dynamic study on stick-slip friction based on non-continuous energy dissipation: *Lubrication Engineering* **2011**, 36(6), 1-3+21.

[17] ABAQUS. ABAQUS analysis user's manual, Version 2016: Dassault Systemes Simulia Corp, 2016.

[18] Polach, O. Creep forces in simulations of traction vehicles running on adhesion limit: *Wear* **2005**, 258(7-8), 992-1000. https//doi.org/10.1016/j.wear.2004.03.046

[19] Wang, X.C., Wang, R.L.; Huang, B.; Mo, J.L.; Ouyang, H.J. A study of effect of various normal force loading forms on frictional stick-slip vibration: *Journal of Dynamics, Monitoring and Diagnostics* **2021**, 1(1), 46-55. https//doi.org/10.37965/jdmd.v2i2.48

[20] Feeny, B.; Guran, A.; Hinrichs, N.; Popp, K. A historical review on dry friction and stick-slip phenomena: *ASME Applied Mechanics Reviews* **1998**, 51(5), 321-341. https//doi.org/10.1115/1.3099008

[21] Li, Z.X.; Cao, Q.J.; Nie, Z.R. Stick-slip vibrations of a self-excited SD oscillator with Coulomb friction: *Nonlinear Dynamics* **2020**, 102, 1419-1435. https//doi.org/10.1007/s11071-020-06009-3

Submitted: 15.09.2023

Accepted: 17.10.2023

Shiyu Liu
[1] The Key Laboratory of Road and Traffic Engineering, Ministry of Education, Shanghai, China
[2] Institute of Rail Transit, Tongji University, Shanghai, China
[3] Shanghai Urban Construction Design & Research Institute (Group) Co., Ltd., Shanghai, China
[4] Shanghai Engineering Research Centre of Tramway, Shanghai, China
Zhiqiang Wang*
Zhenyu Lei
Institute of Rail Transit, Tongji University, Shanghai, China
*Corresponding author:
18621802301@163.com